MECHANIKA TEORETYCZNA
I STOSOWANA
Journal of Theoretical
and Applied Mechanics
4, 33, 1995

TORSIONAL VIBRATION CONTROL BY ACTIVE PIEZOELECTRIC SYSTEM

PIOTR M. PRZYBYŁOWICZ

Institute of Machine Design Fundamentals

Warsaw University of Technology

The basic electromechanical properties of piezoelectric material-lead zirconate titatnate (PZT) are mentioned in the paper in terms of their usability to damp torsional vibration of shafts. Piezoceramics exhibit natural shear effect being three times as much as the longitudinal one. This phenomenon can successfully be utilized in torsional systems for vibration control as piezoceramics constitute perfect elements for actuator applications. Active control is achieved through closed loop with proportional and velocity feedback. The objective of the analysis is to determine the efficiency of electronic damping. The model is developed to include actuator inertia since PZTs possess mass density of level similar to that of steel. Disturbances concomitant with dynamic behaviour of the system due to imperfect actuator bonding to the shaft surface by a glue layer are also taken into account.

1. Introduction

Piezoelectric materials made of lead zirconate titanate ceramics (PZT) are known to reveal natural shear effect, i.e., which appears under electric field applied along the principal anisotropy axes. This effect is strong, compared to longitudinal one, roughly, three times greater. It makes PZT ceramics the ideal elements for actuator applications in torsional systems in which vibration amplitude reduction is crucial for their proper performance. Technical motivation that may encompass the advantages of piezoceramic materials is also concerned with problems of micropositioning in robotics, adaptive systems of the mirrors in astronomic measurements (Rogers (1993)), metrology, etc. Meng-Kao Yeh and Chih-Yuan Chin (1994) proved the applicability of piezoelectric sensors for measuring torsional vibration of shafts.

Introductory theoretical studies of shafts vibration induced by piezoelements based on PZT ceramics were presented by Kurnik and Przybyłowicz (1995). Experimental investigations dealing with actively controlled torsional system were carried out by Chia-Chi Sung et al. (1994). Nonetheless, the analytical study is still to be set forth. The present work is intended to undertake this effort. Moreover, the model of the system is to be completed with the actuator inertia. The bonding interlayer of glue is no longer rigid and cannot secure the perfect attachment between the piezoelements and shaft surface. It seems interesting to assess the extent to what those effects can disturb the dynamics of the system – in other words, to state whether they are negligible or not. Analogous problems were widely discussed in the case of beam-like systems by Crawley and de Luis (1987) who regarded different types of physical connection between beams and actuators. The influence of bonding interlayer was also poinetd out in works by Tylikowski (1993).

2. Basic assumptions

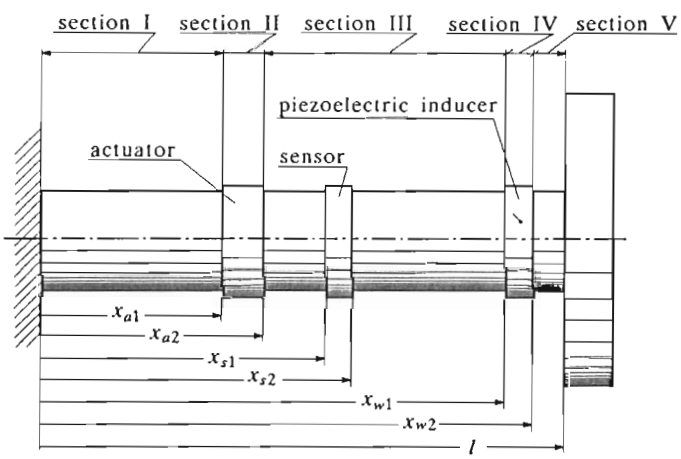

Fig. 1. Model with sectional segmentation

The considered model is presented in Fig.1. It consists of a thin-walled shaft with additional lumped inertia (a disc) mounted to its geometrically free end. The shaft is equipped with three piezoelectric elements: sensor, actuator and inducer. The sensor is also made of PZT, yet it is to be thin enough to

be neglected in total inertia balance of the system. The actuator is posed by a ring-shaped element of considerable thickness, thus its moment of inertia must be taken into account. Such assumption is escaped by the piezoelectric inductor which serves here only as formal element to excite the system by the action of a pair of harmonic-type and out-of-phase concentrated torques. Its mass is not to affect the system dynamics since real systems may not be excited that way. Consistently, the model breaks up into five sections which have to satisfy physical continuity conditions. The sensor and the actuator are electronically coupled with proportional and velocity feedback ruling the performance of thus arranged control system.

The analysis will be done within linear theory. Hence, the bonding interlayer of glue is modelled by perfectly elastic material. In order to put a special emphasis on electronic damping efficiency itself the rheological properties (internal friction) of all the materials involved are excluded.

3. Governing formulae and equations of motion

Theoretical grounds on which the performance of piezoelectric materials is governed can be expressed in terms of their constitutive equations. For typical piezoelectrics the first-order approximation of these equations has the form (cf Damjanović and Newnham (1992))

$$\varepsilon_{ij} = s_{ijkl}^{(E)}\sigma_{kl} + d_{ijk}E_k \tag{3.1}$$

$$D_i = d_{ijk}\sigma_{jk} + \epsilon_{ij}^{(\sigma)}E_j \tag{3.2}$$

where σ_{kl} and E_k are the components of the stress tensor and the electric field vector respectively. The coefficients $s_{ijkl}^{(E)}$ are the components of the elastic compliance tensor measured at a constant electric field. The components d_{ijk} and $\epsilon_{ij}^{(\sigma)}$ denote linear electromechanical coupling and dielectric permittivity measured under constant stress. Because of the symmetry of the stress and strain tensors the third rank tensor d_{ijk} is also symmetrical in indices j and k (which leaves only 18 independent coefficients). This makes it possible to derive a simplier, matrix form notation of Eqs (3.1) and (3.2) by incorporating the index formula: $ii \to i$, and: $23(32) \to 4$, $13(31) \to 5$, $12(21) \to 6$.

By applying the ring-type actuator (terminology due to Chia-Chi Sung et al. (1994)), as it can be seen in Fig.2, one can derive from the matrix version of constitutive equations the following formula, henceforth called the actuator

law:

$$\tau_{pe} = G_{pe}\left[(R + t_s)\frac{\partial \varphi_{pe}}{\partial x} - 2\frac{d_{15}}{h_e}U_A\right] \tag{3.3}$$

where

τ_{pe}, G_{pe} – shear stress and shear modulus of PZT material
h_e – width of the actuator
U_A – applied voltage
$R + t_s$ – inner actuator radius (glue layer of t_s thickness included).

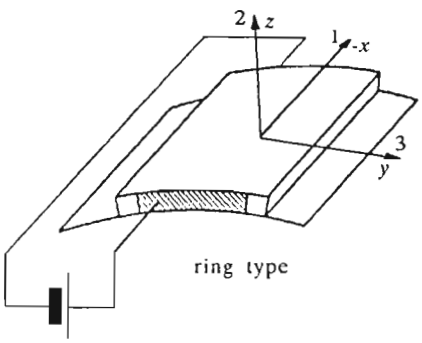

Fig. 2. Ring-type actuator – the principal anisotropy axes

The torque produced by the actuator can be calculated by integrating the shear stress τ_{pe} over the entire cross-section of the piezoelement. On the assumption of constant stress distribution one obtains

$$M_A = \frac{4d_{15}}{3h_e}U_A\left[(R + t_s + h_{pe})^3 - (R + t_s)^3\right]G_{pe} \tag{3.4}$$

Voltage applied to the actuator as well as its growth ratio, appropriately amplified, comes from the sensor according to assumed feedback

$$U_A = k_p U_S + k_d \frac{\partial U_S}{\partial t} \tag{3.5}$$

where the subscripts A and S stand for the actuator and sensor, k_d, k_p are the gain factors introduced by the electronic circuit. Making use of the constitutive equations we can find the voltage produced by the sensor. Lee (1990) and Tzou (1991) came up with the following reasoning to determine the amount of electric charge generated by the sensor

$$Q = \oint_A D\, dA \tag{3.6}$$

where

D – dielectric displacement

dA – elementary sensor area.

For convenience, the subscripts denoting electric field direction are omitted. Eq (3.6), of course, yields $Q = 0$ since the sensor as typical capacitor accumulates equal charge in each plate, yet of opposite sign. Nonetheless, classical formula for flat condensers makes it possible to find the voltage swept by the sensor. After transformations the final result can be written as

$$U_S = \frac{G_{pe} d_{15} R}{\epsilon_0 \epsilon_{pe}} \left[\varphi_{pe}(x_{s2}, t) - \varphi_{pe}(x_{s1}, t) \right] \tag{3.7}$$

where ϵ_0, ϵ_{pe} are the absolute and relative dielectric permittivity of PZT respectively, and $\varphi_{pe}(\cdot)$ denotes current angular displacement of the sensor at x_{s1} and x_{s2} coordinates (see Fig.1). Eqs (3.4) and (3.7) coupled by Eq (3.5) create the theoretical description of the control system work. Another problem to be analyzed is posed by mechanical interactions between the shaft and piezoelements attached to it. Motion of the actuator is induced by shaft vibration through deformable layer of glue. It is then desired to derive the equation of motion corresponding to section II (see Fig.1) where bonding layer influence is of high interest. Let us consider the infinitesimal segment of length dx which belongs to this section.

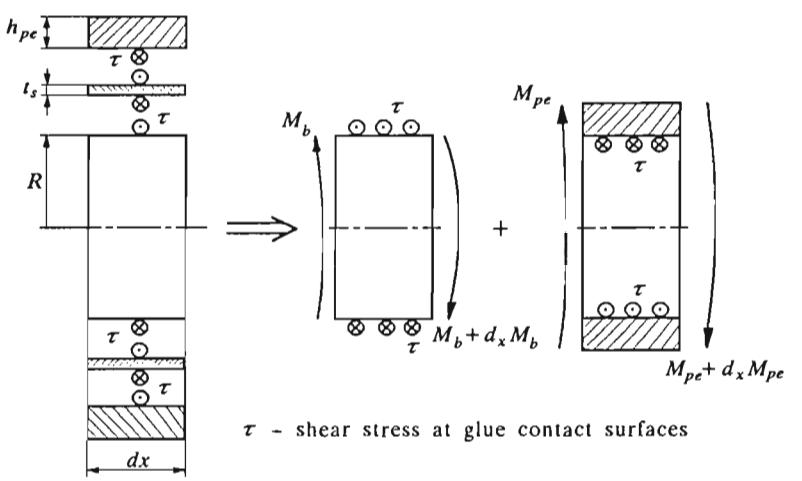

Fig. 3. Infinitesimal segment of shaft and actuator, glue layer included

Equation of motion for the shaft segment is

$$dI_b \frac{\partial^2 \varphi_b}{\partial t^2} = d_x M_b + 2R^2 \tau_s dx$$
$$M_b = G_b J_b \frac{\partial \varphi_b}{\partial x} \tag{3.8}$$

where

I_b, J_b – mass and geometric moment of inertia, respectively
G_b – shear modulus
φ_b – angular displacement
M_b – internal torque
τ_s – shear stress measured at the inner and outer surface of glue.

The analogous equation for the actuator segment is given by

$$dI_{pe} \frac{\partial^2 \varphi_{pe}}{\partial t^2} = d_x M_{pe} - 2(R + t_s)^2 \tau_s dx$$
$$M_{pe} = G_{pe} J_{pe} \frac{\partial \varphi_{pe}}{\partial x} \tag{3.9}$$

where the subscript pe refers to "piezoelectric". Eqs (3.8) and (3.9) are coupled by the term τ_s. Decoupling of these equations can be obtained having τ_s explicitly resolved first. Let us consider the shear strain of the glue layer to evaluate the corresponding stress. Deformation of the glue is shown in Fig.4.

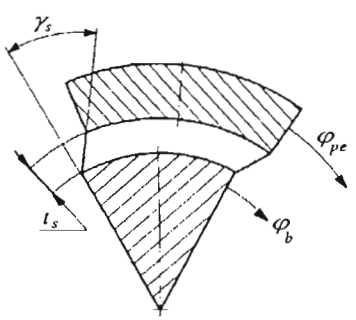

Fig. 4. Deformation of glue layer

Geometric relations for small values of angular displacements φ_b, φ_{pe} directly lead to the following equation

$$\gamma_s = \frac{1}{t_s}\left[(R + t_s)\varphi_{pe} - R\varphi_b\right] \qquad \tau_s = G_s \gamma_s \tag{3.10}$$

where G_s is the shear modulus of the gluing material. By introducing formula (3.10) to Eqs (3.8) and (3.9) we obtain equation which can be conscisely written as

$$\rho_k \frac{\partial^2 \varphi_k}{\partial t^2} - G_k \frac{\partial^2 \varphi_k}{\partial x^2} + (-1)^{\delta_{kb}} \frac{2G_s}{J_k t_s}(R + t_s \delta_{k\,pe})\Big[(R + t_s)\varphi_{pe} - R\varphi_b\Big] = 0 \tag{3.11}$$

$$k = b, pe$$

where $\delta_{k(\cdot)}$ denotes the Kronecker delta. By extraction of φ_{pe} from Eqs (3.11) at $k = b$ and differentiating twice thus obtained expression with respect to t and x, then substituting to Eqs (3.11) again, yet when $k = pe$, we finally get the uncoupled equation of the shaft motion. It has the following form

$$\begin{aligned} &G_b G_{pe} J_b J_{pe} \frac{\partial^4 \varphi_b}{\partial x^4} - J_b J_{pe} t_s (G_b \rho_{pe} + G_{pe} \rho_b) \frac{\partial^4 \varphi_b}{\partial x^2 \partial t^2} + \\ &-2G_s \Big[G_{pe} J_{pe} R^3 + G_b J_b (R + t_s)^3\Big] \frac{\partial^2 \varphi_b}{\partial x^2} + \\ &+2G_s \Big[\rho_{pe} J_{pe} R^3 + \rho_b J_b (R + t_s)^3\Big] \frac{\partial^2 \varphi_b}{\partial t^2} + \rho_b \rho_{pe} J_b J_{pe} \frac{\partial^4 \varphi_b}{\partial t^4} = 0 \end{aligned} \tag{3.12}$$

Assuming harmonic excitation, the steady-state solution can be predicted in the form

$$\varphi_b(x, t) = \Phi_b(x) \exp(\mathrm{i}\omega t) \tag{3.13}$$

where ω is the excitation frequency.

Substitution of Eq (3.13) into Eq (3.12) leads to the ordinary differential equation of the fourth order. To solve it we put

$$\Phi_b(x) = \exp(kx) \tag{3.14}$$

which yields the characteristic polynomial. It is a biquadratic one with respect to k

$$a_4 k^4 + a_2 k^2 + a_0 = 0 \tag{3.15}$$

where a_4, a_2, a_0 can be found from Eq (3.12). It occurs that for the given set of material and geometrical data the discriminant of Eq (3.15) is always positive and the product of roots $k_1^2 \cdot k_2^2$ negative. Having this stated it is convenient to introduce the final form of the characteristic equation roots

$$\begin{aligned} k_1 &= \mathrm{i}\sqrt{k_1^2} = \mathrm{i}q(\omega) & k_3 &= \sqrt{k_2^2} = p(\omega) \\ k_2 &= -\mathrm{i}\sqrt{k_1^2} = -\mathrm{i}q(\omega) & k_4 &= -\sqrt{k_2^2} = -p(\omega) \qquad p, q > 0 \end{aligned} \tag{3.16}$$

Finally, the solution of Eq (3.12) can be written as

$$\varphi_b(x,t) = \left[\tilde{C}_1 \exp(\mathrm{i}qx) + \tilde{C}_2 \exp(-\mathrm{i}qx) + \tilde{C}_3 \exp(px) + \right. \\ \left. + \tilde{C}_4 \exp(-px)\right] \exp(\mathrm{i}\omega t) \tag{3.17}$$

where $\tilde{C}_1, ..., \tilde{C}_4$ are complex constants. It is to be noted that x coordinate is measured from the beginning point of the second section which corresponds to coordinate x_{a1}. For finding the general solution, where x is zero at the fixed end of the shaft we can transform Eq (3.17) to obtain

$$\varphi_b(x,t) = \Big(C_1 \cos[q(x - x_{a1})] + C_2 \sin[q(x - x_{a1})] + \\ + C_3 \exp[p(x - x_{a1})] + C_1 \exp[-p(x - x_{a1})]\Big) \sin \omega t \tag{3.18}$$

where, in turn, $C_1, ..., C_4$ are real constants.

Equations of motion for all the rest shaft sections are identical

$$\rho_b \frac{\partial^2 \varphi_b}{\partial t^2} - G_b \frac{\partial^2 \varphi_b}{\partial x^2} = 0 \tag{3.19}$$

Their solutions can be expressed as

$$\varphi_j(x,t) = \sum_{k=1}^{2} \tilde{C}_{jk} \exp[(-1)^k a(x - x_j)] \exp(\mathrm{i}\omega t) \qquad j = 1,3,4,5 \tag{3.20}$$

where $a = \omega\sqrt{\rho_b/G_b}$ and x_j are the beginning coordinates corresponding to those sections.

4. Boundary conditions

Dynamics of the entire system is reflected by formulae (3.18) and (3.20). They introduce twelve constants to be determined by applying boundary conditions. These must satisfy physical continuity of the system and also regard the external excitation as well as the limitations imposed on the actuator work. All the conditions are given below:

1. Angular displacement at the fixed end

$$\varphi_1(0,t) = 0$$

2. Angular displacements and internal moments compatibility at the section boundaries abutting on the actuator section

$$\varphi_1(x_{a1},t)-\varphi_2(x_{a1},t)=0 \qquad \varphi_{1,x}(x_{a1},t)-\varphi_{2,x}(x_{a1},t)=0$$
$$\varphi_2(x_{a2},t)-\varphi_3(x_{a2},t)=0 \qquad \varphi_{2,x}(x_{a2},t)-\varphi_{3,x}(x_{a2},t)=0$$

where the subscript preceded by the comma denotes derivative with respect to indicated symbol

3. Compatibility of angular displacements for the rest of the sections and external moments application

$$\varphi_3(x_{w1},t)-\varphi_4(x_{w1},t)=0 \qquad \varphi_{3,x}(x_{w1},t)=-\varphi_{4,x}(x_{w1},t)=\frac{M(t)}{G_bJ_b}$$

$$\varphi_4(x_{w2},t)-\varphi_5(x_{w2},t)=0 \qquad \varphi_{4,x}(x_{w2},t)=-\varphi_{5,x}(x_{w2},t)=-\frac{M(t)}{G_bJ_b}$$

where $M(t)$ denotes the amplitude of excitation torque

4. No shear stress at the free side surfaces of the actuator

$$\tau_{pe}(x_{a1},t)=0 \qquad \tau_{pe}(x_{a2},t)=0$$

5. Lumped moment of inertia at the end of the shaft

$$I_d\varphi_{5,tt}(\ell,t)+G_bJ_b\varphi_{5,x}(\ell,t)=0$$

Generally, we obtain the set of 12 simultaneous linear equations in 12 unknows $C_1,\ldots,C_{12}$. The presence of differential element in the control system (velocity feedback) implies complex solution of $C_1,\ldots,C_{12}$. Hence

$$C_j(\omega)=c_j(\omega)+\mathrm{i}v_j(\omega) \qquad \mathrm{i}=\sqrt{-1} \quad j=1,\ldots,12 \tag{4.1}$$

The shaft vibration amplitude at a given location, e.g., at $x=\ell$ (geometrically free end), as real value, can be found in the following form

$$\begin{aligned} A=\Phi_5(\ell) \;=\; & \Big\{\Big(c_{11}\cos[q(\ell-x_{w2})]+c_{12}\sin[q(\ell-x_{w2})]\Big)^2+ \\ & +\Big(v_{11}\cos[q(\ell-x_{w2})]+v_{12}\sin[q(\ell-x_{w2})]\Big)^2\Big\}^{\frac{1}{2}} \end{aligned} \tag{4.2}$$

Eq (4.2) enables one to draw the amplitude-frequency characteristics reflecting dynamic behaviour of the entire system.

5. Numerical results

By developing the model with additional inertia due to piezoelectric element it is possible to discuss its influence on the entire system behaviour. As expected, massive actuator decreases resonant frequencies, and this decrement can be of considerable value for thin shafts or those made of plastics (for instance, Chia-Chi Sung et al. experimentally studied phenolic and pyrex glass tubes). The system dynamics becomes even more complicated if deformation of the glue is taken into account. Gluing materials of low Kirchhoff's modulus $\sim 10^7$ MPa can definitely disturb amplitude-frequency characteristics. The actuator attached to the shaft by elastic layer exhibits properties analogous to classical passive vibration eliminator, which makes it necessary to consider this side-effect in system tuning, i.e. selecting its basic parameters. The influence of glue shear stiffness on amplitude-frequency characteristics for inactivated control system is presented in Fig.5.

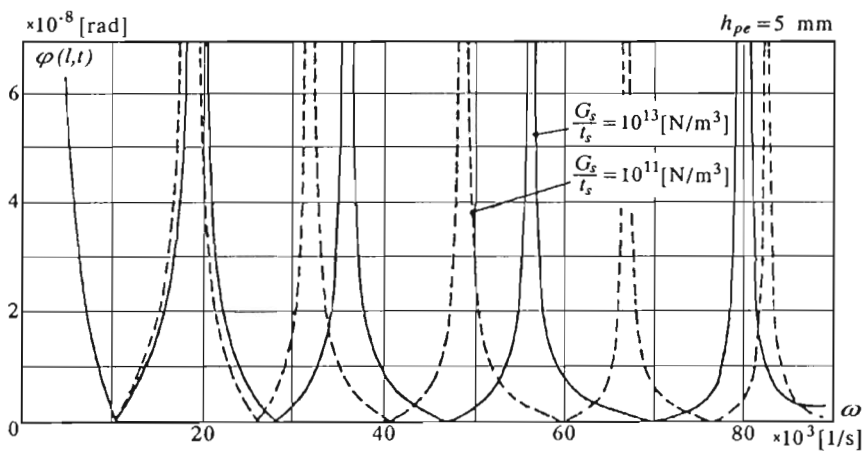

Fig. 5. Influence of glue layer stiffness

The problems relevant to active control with actuator inertia and bonding layer elasticity included stay no longer as simple as in the case of typical formulation where these side-effects are omitted. Now, it is not sufficient to determine modal functions to discuss their controllability by the active system. It occurs that different materials of glue or piezoelectrics can highly affect the efficiency of the control. Consider the following graphs given in Fig.6 ÷ Fig.8.

The characteristics reveal damping properties of the system for some exemplary locations of the actuator. All of them are obtained for very stiff glue

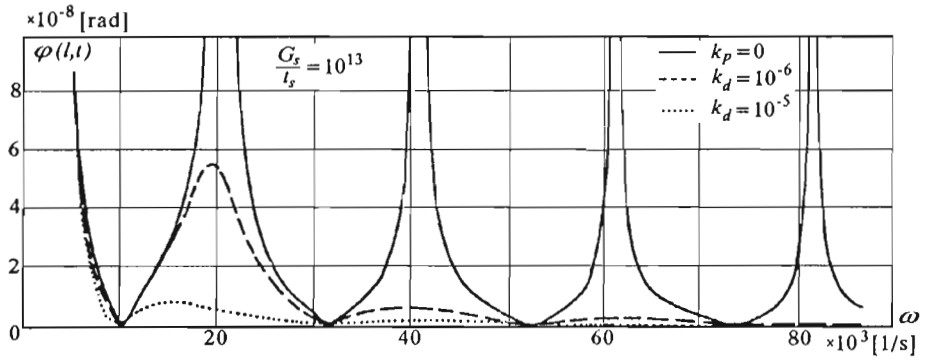

Fig. 6. Amplitude-frequency characteristics with activated control system. Actuator position $x_{a1} = 0$

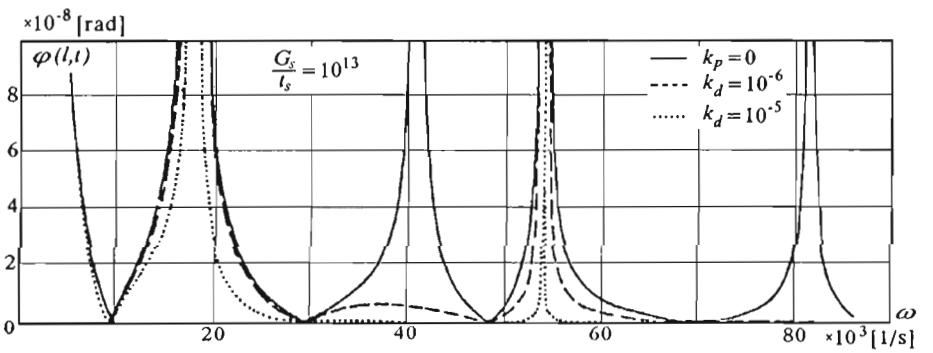

Fig. 7. Active control at $x_{a1} \approx 1/2$ of the shaft length

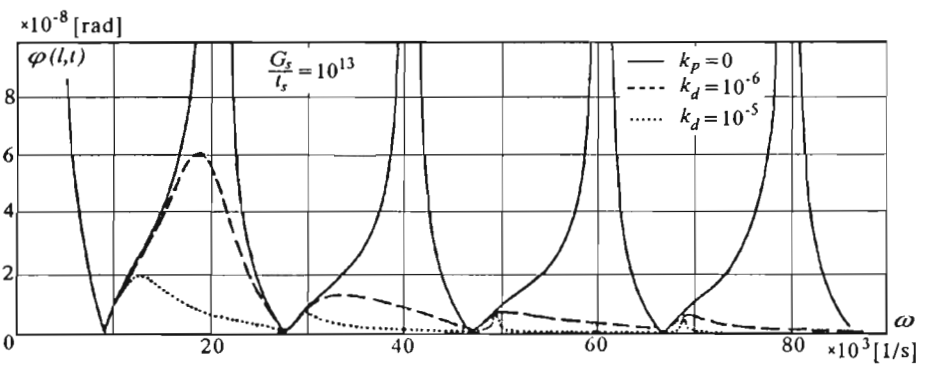

Fig. 8. Active control at $x_{a1} \approx \ell$

layer (almost perfect bonding). It can be seen that the efficiency of damping reaches its maximum for actuator locations near the fixed end of the shaft. Quite good properties exhibits collocated sensor/actuator system positioned close to the free end. As an instance, middle actuator location results in non-controllability of the second and fourth mode. The situation is changed if a "soft" kind of the glue is employed. The efficiency of collocated system at the free end is not as good as before. Now, the most preferable locations of actuator application are to be found at $\sim 1/4$ of the shaft length. Non-controllability "shifts" from the fourth to third mode (see Fig.7 and Fig.9).

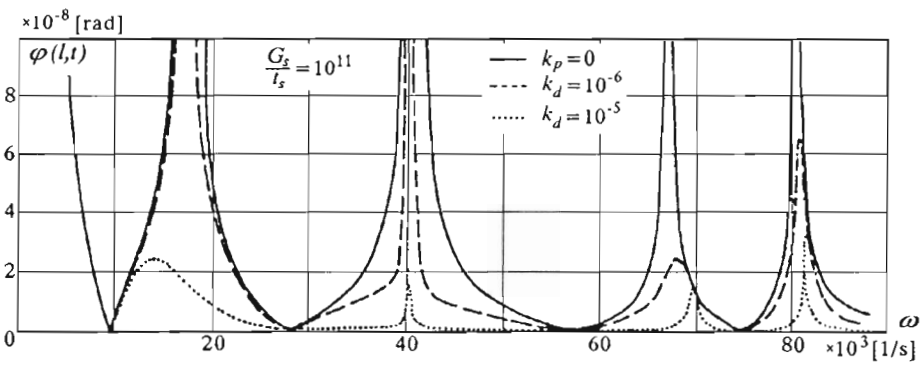

Fig. 9. Damping efficiency for "soft" glue, $x_{a1} \sim 1/\ell$

Naturally, sufficiently high values of amplification coefficients k_p and k_d stifle those side-effects. Still, it is interesting to resolve what kind of feedback is more effective. Proportional or velocity one? The problem is especially vivid in the hardest to damp, the first mode. For this purpose some characteristics obtained for different conditions are presented, see Fig.10 and Fig.11. Velocity feedback gives desired effects for $k_d = 0.001 \div 0.01$. It holds true in the case of "soft" glue and different points of actuator application. Some troubles appear in the case of proportional feedback exclusively, where the control with stiff glues incorporated tends to maintain high vibration amplitudes, yet peaking at higher frequencies. Effective damping, critical with respect to first mode as well, can be achieved at considerable gain factors k_p. Such a situation is undesired since it hazards the control system by exposing it to high voltages. It is to be noted that PZT ceramics do not possess impressive dielectric strength, compared to, e.g., PVDF organic films. Besides, high gain factors jeopardize the safety of the electronic circuit.

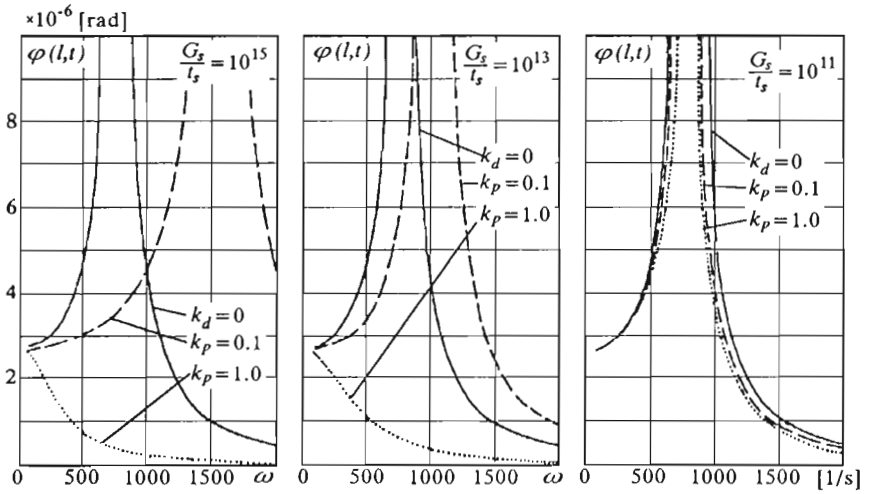

Fig. 10. First mode damping. Proportional feedback

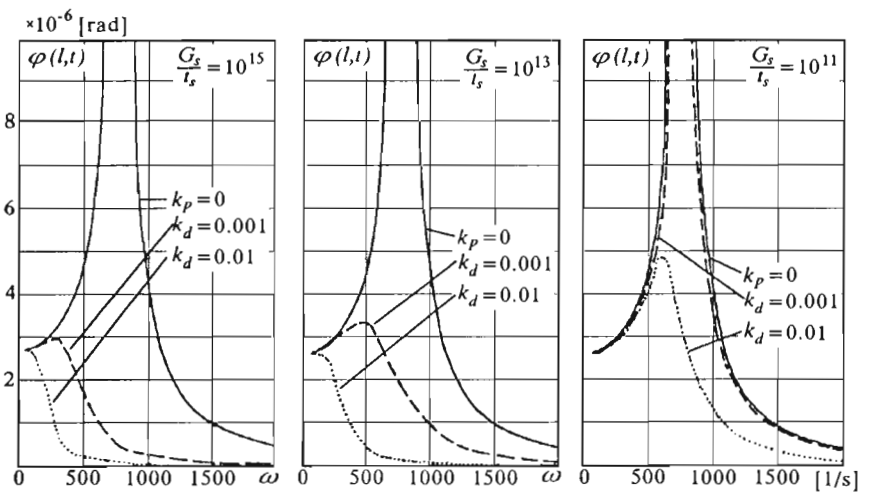

Fig. 11. First mode damping. Velocity feedback

6. Concluding remarks

Active control by piezoelectric elements proves to be a powerful tool in reducing vibration amplitude of torsional systems. Application of the electronic damping gives excellent results, especially in control systems governed by velocity feedback, even for different points of actuator application and spatial sensor/actuator dislocation. This is highly important since real technical conditions may not always allow arbitrary piezoelements application. The work emphasizes some aspects related to the active control under more realistic conditions. The model is burdened with piezoelement inertia and the bonding interlayer of glue remains no longer perfect.

Acknowledgement

The author wishes to thank Prof. Tylikowski for including him in his research program supported by the State Committee for Scientific Research (Grant KBN – No. 3P40400907)

References

1. CHIA-CHI SUNG, VASUNDARA V. VARADAN, XIAO-QI BAO, VIJAY K. VARADAN, 1994, Active Torsional Vibration Control Experiments Using Shear-Type Piezoceramic Sensors and Actuators, *Journal of Intelligent Material Structures and Systems,* **5**, 3, 436-442

2. CRAWLEY E.F., DE LUIS J., 1987, Use of Piezoelectric Actuators as Elements of Intelligent Structures, *American Institute of Aeronautics and Astronautics Journal,* **25**, 1373-1385

3. DAMJANOVIĆ D., NEWNHAM R.E., 1992, Electrostrictive and Piezoelectric Materials for Actuator Applications, *Journal of Intelligent Material Structures and Systems,* **3**, 4, 190-208

4. KURNIK W., PRZYBYŁOWICZ P.M., 1995, Torsional Vibration of a Tube with Piezoelectric Actuators, *Zeitschrift für Angewandte Mathematik und Mechanik,* **75**, 1 , S55-S56

5. LEE C.K., 1990, Theory of Laminated Piezoelectric Plates for the Design of Distributed Sensors/Actuators. Part I: Governing Equations and Reciprocal Relationships, *Journal of Acoustical Society of America,* **87**, 3, 1144-1158

6. MENG-KAO YEH, CHIH-YUAN CHIN, 1994, Dynamic Response of Circular Shaft with Piezoelectric Sensor, *Journal of Intelligent Material Structures and Systems,* **5**, 11, 833-840

7. ROGERS C.A., 1993, Intelligent Material Systems – The Dawn of a New Materials Age, *Journal of Intelligent Material Structures and Systems,* **4**, 1, 4-12

8. TYLIKOWSKI A., 1993, Dynamics of Laminated Beams with Active Fibers, *Proceedings of the 3rd Polish-German Workshop on Dynamical Problems in Mechanical Systems,* Edit. R.Bogacz and K.Popp, 67-78

9. TYLIKOWSKI A., 1993, Stabilization of Beam Parametric Vibrations, *Journal of the Theoretical and Applied Mechanics,* **31**, 3, 657-670

10. TZOU H. S., 1991, Distributed Piezoelectric Neurons and Muscles for Shell Continua, *The 1991 ASME Design Technical Conferences – 13th Biennial Conference on Mechanical Vibration and Noise, Structural Vibration and Acoustics,* DE-Vol. 34, 1-6

Aktywne sterowanie drgań skrętnych za pomocą układu piezoelektrycznego

Streszczenie

W pracy przedstawiono elektromechaniczne właściwości piezoelektryka wykonanego ze spieków tlenku cyrkonu i tytanu (PZT) w kontekście ich przydatności do tlumienia drgań skrętnych walów. Piezoceramiki wykazują naturalny efekt postaciowy, będący trzykrotnie większy niż efekt wzdłużny. Zjawisko to może być z powodzeniem wykorzystane w układach skrętnych, gdyż piezoelektryki te znakomicie nadają się do zastosowania jako elementy wykonawcze do sterowania drganiami. Aktywne sterowanie uzyskuje się poprzez zamknięcie pętli sprzężenia zwrotnego z proporcjonalnym i różniczkującym układem regulacji. Celem analizy jest ocena skuteczności tlumienia elektronicznego. Rozważany model jest wzbogacony o uwzględnienie bezwładności, jaką wprowadza element wykonawczy PZT, gdyż gęstość piezoceramików jest zbliżona do gęstości stali. Towarzyszące zaburzenia dynamiki układu wskutek niedoskonałego połączenia elementu wykonawczego z walem poprzez warstwę kleju również wzięto pod uwagę.

Manuscript received March 1, 1995; accepted for print April 6, 1995